AIP | Journal of Applied Physics

Molecular dynamics studies of the bonding properties of amorphous silicon nitride coatings on crystalline silicon

Keith T. Butler, Machteld P. W. E. Lamers, Arthur W. Weeber, and John H. Harding

Citation: J. Appl. Phys. **110**, 124905 (2011); doi: 10.1063/1.3670068
View online: http://dx.doi.org/10.1063/1.3670068
View Table of Contents: http://jap.aip.org/resource/1/JAPIAU/v110/i12
Published by the American Institute of Physics.

Related Articles

Photon ratchet intermediate band solar cells
Appl. Phys. Lett. 100, 263902 (2012)

A physics-based model of the electrical impedance of ionic polymer metal composites
J. Appl. Phys. 111, 124901 (2012)

Interplay of bulk and surface properties for steady-state measurements of minority carrier lifetimes
J. Appl. Phys. 111, 123703 (2012)

Resolving the ultrafast dynamics of charge carriers in nanocomposites
Appl. Phys. Lett. 100, 241906 (2012)

Ultrafast carrier dynamics and radiative recombination in multiferroic BiFeO3
Appl. Phys. Lett. 100, 242904 (2012)

Additional information on J. Appl. Phys.

Journal Homepage: http://jap.aip.org/
Journal Information: http://jap.aip.org/about/about_the_journal
Top downloads: http://jap.aip.org/features/most_downloaded
Information for Authors: http://jap.aip.org/authors

ADVERTISEMENT

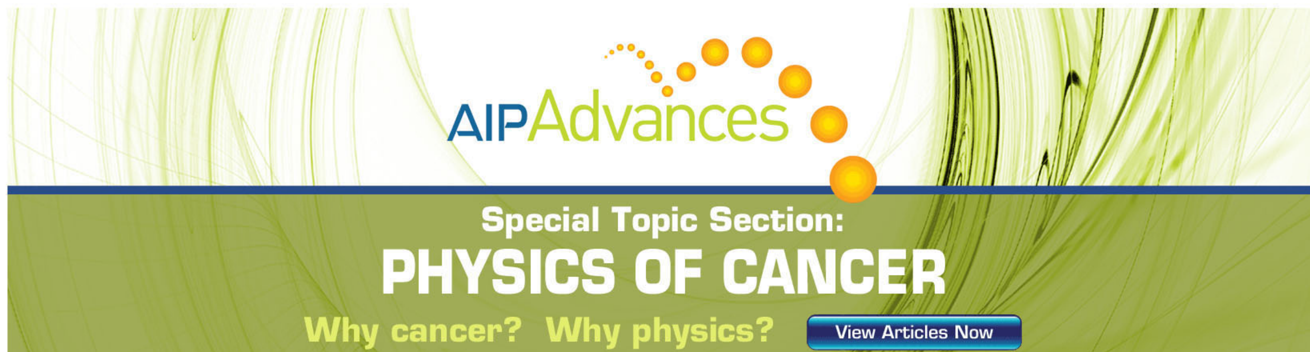

Downloaded 02 Jul 2012 to 130.112.1.3. Redistribution subject to AIP license or copyright; see http://jap.aip.org/about/rights_and_permissions

JOURNAL OF APPLIED PHYSICS 110, 124905 (2011)

Molecular dynamics studies of the bonding properties of amorphous silicon nitride coatings on crystalline silicon

Keith T. Butler,[1,a)] Machteld P. W. E. Lamers,[2] Arthur W. Weeber,[2] and John H. Harding[1]
[1]*Department of Materials Science and Engineering, Sir Robert Hadfield Building, Mappin Street, Sheffield, S13JD, United Kingdom*
[2]*ECN Solar Energy, NL-1755 ZG, Petten, The Netherlands*

(Received 21 June 2011; accepted 5 November 2011; published online 20 December 2011)

In this paper we present molecular dynamics simulations of silicon nitride, both in bulk and as an interface to crystalline silicon. We investigate, in particular, the bonding structure of the silicon nitride and analyze the simulations to search for defective geometries which have been identified as potential charge carrier traps when silicon nitride forms an interface with silicon semiconductors. The simulations reveal how the bonding patterns in silicon nitride are dependent upon the stoichiometry of the system. Furthermore we demonstrate how having an "interphase", where the nitrogen content in silicon gradually reduces toward pure silicon across a boundary region, as opposed to an interface where there is an abrupt drop in nitrogen concentration at the boundary, can result in significantly different numbers of certain important carrier trap. © *2011 American Institute of Physics*. [doi:10.1063/1.3670068]

I. INTRODUCTION

The deposition of amorphous silicon nitride (SiN_x) on silicon semiconductors in photovoltaic cells has become a popular strategy for a number of reasons. Initially SiN_x layers were introduced for the formation of metal-insulator-semiconductor structures.[1] In solar cells they were first used due to their properties as an anti-reflective coating (ARC). The presence of an ARC in crystalline silicon (c-Si) solar cells is important as a clean c-Si surface reflects more than 35% of incident light. The presence of an ARC allows for effective utilization of this light. That the inclusion of a SiN_x layer increases the performance of solar cells by more than would be expected merely from its role as an ARC has been explained by its ability to reduce the rate at which excess charge carriers recombine at the semiconductor surface,[2] a property known as passivation. Thus SiN_x coatings address the two major loss mechanisms in solar cells, namely optical and electrical losses. Due to these dual beneficial properties for the improvement of photovoltaics as well as its importance in metal-oxide-semiconductor field effect transistors (MOSFETs) the silicon/silicon nitride interface has been the subject of much research since the early 1990 s.[3–5]

Much of the work done on ARC development to date has focused on finding the optimal ratio of N to Si (i.e., the value of x in SiN_x in the layer) in order to maximize the percentage of incident light trapped in the c-Si layer.[6] There is a balance to be achieved between reducing reflection (this is minimized by increasing the refractive index (n) of the ARC) and reducing the amount of light absorbed by the ARC. One problem is that in order to reduce the amount of light absorbed in the ARC it is necessary to reduce the number of Si-Si and Si-H bonds (i.e., higher values of x), however to increase the refractive index lower values of x are desirable. If one were to ignore the effects of absorption of light a value of $n = 2.3–2.4$ would be optimal. The optimal value of x and hence n, is very dependent upon the type of solar cell, the optimal wavelength, the texture, the module fabrication etc, for example, in air a value of $n = 1.9$ is optimal, however generally in solar cells in modules values of $n = 2.04 - 2.08$ are preferred.[7,8]

Although much of the attention in the development of SiN_x layers for high performance solar cells has been focused on the optimization of the two roles as an ARC and a passivation layer[9–14] it is only recently that the interrelatedness of these two functions has been elucidated. Jung *et al.*[15] performed a comprehensive study of bandgap and defect effects in amorphous silicon nitride (a-SiN_x), indicating the important role of these effects in determining the efficiency of a solar cell.

There has been a lot of experimental work done in characterizing the stoichiometric $Si(111)/Si_3N_4$ interface. Much of this effort has concentrated on identifying the types of surface reconstruction and charge transfers involved at the interface. 7×7,[5] 4×4,[16] $8/3 \times 8/3$,[17] and 8×8^3 reconstructions have all been observed. The $Si(100)/SiN_x$ interface has been studied by electron paramagnetic resonance (EPR),[18] which revealed the major electron trap in the interface layer to be due to under-coordinated Si. Further studies of this interface with transmission electron microscopy (TEM) showed that N atoms were present on the c-Si side of the interface up to the second layer.[19] Such penetration of N, into the c-Si layer is also known to be extremely sensitive to the conditions during the deposition of the ARC.[8]

In a-SiN_x a number of geometrical defects have been identified that have important implications for the electronic structure, two of the most important, the so-called K and N defects are shown in Fig. 1. The K center consists of a Si bound to three N atoms with a dangling bond ($N_3 \equiv Si$) and is observable by electron spin resonance (ESR).[20] A defect center due to an under coordinated N atom ($Si_2 = N$) has

a)Electronic mail: K.Butler@sheffield.ac.uk.

 © 2011 American Institute of Physics

Downloaded 02 Jul 2012 to 130.112.1.3. Redistribution subject to AIP license or copyright; see http://jap.aip.org/about/rights_and_permissions

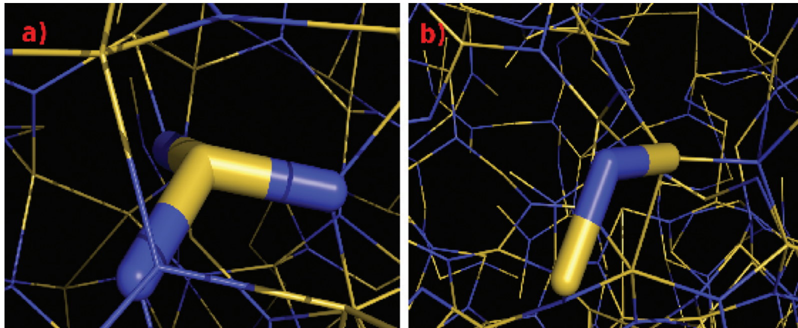

FIG. 1. (Color online) Important defect geometries in the SiN_x layer. (a) The K-defect, where Si is bonded to three N atoms with one dangling bond. (b) The N defect, where N is bonded to two Si atoms with one dangling bond.

also been observed.[21] These assignments have also been supported by *ab initio* calculations.[22]

In this paper we simulate the Si(100) interface in contact with SiN_x:H at an atomistic level. SiN_x:H layers with $x = 0.8$, 0.9,1. 0, 1.1, and 1.2, incorporating 20 at. % H are simulated. For each value of x, we simulate both a clean interface, with an abrupt SiN_x:H/c-Si partition and a gradual interface with a gradient of x across a distance of 20 Å. We shall refer to these interfaces as clean and gradual interfaces, respectively. We perform a topological analysis of the trajectories generated in our molecular dynamics (MD) simulations. We calculate the radial distribution functions (RDFs) for bulk SiN_x comparing to previous theoretical work, as a validation of our method and investigate bonding patterns in the interfacial regions of our models to identify and quantify defect centers, revealing a clear difference in the frequency of occurrence and degree of passivation of K and N defects at clean and gradual interfaces.

II. METHODS

A. Generating amorphous SiN_x

All interactions in the system were modeled using Tersoff type potentials.[23] We use the parameterization of these potentials developed by de Brito Mota *et al.*,[24] which were previously used to simulate amorphous SiN_x (Ref. 24) and SiN_x:H.[25] All MD simulations presented in this paper were run using the DLPOLY code.[26]

The first step in our procedure is to generate samples of a-SiN_x. This is achieved by randomly placing Si and N atoms in a simulation cell, subject to certain interatomic separation criteria, in the correct ratio. The cell volumes were set by estimation of the required density, from a linear interpolation between the density if c-Si and c-Si_3N_4. The details of the simulation cells are presented in Table I.

TABLE I. Numbers of atoms in the simulation cells used to generate the a-SiN_x.

x	Si Atoms	N Atoms	H Atoms	Density (g/cc)
0.8	415	332	187	2.86
0.9	409	368	194	2.92
1.0	404	404	202	2.98
1.1	400	440	210	3.04
1.2	394	473	217	3.10

In order to generate the amorphous samples, the initially random configurations were run at 2500 K for 0.5 ns with a time step of 1 fs in the constant volume canonical (NVT) ensemble. After this simulation, the systems were then quenched to 350 K at a rate of 3×10^{11} K/s. We tested various quenching rates on samples of a-Si_3N_4 and found that this was the fastest rate at which no significant increase in the number of defects present in the sample was observed, compared to quicker rates.

We then add 20 at. % H (Table I) to the simulation cells and equilibrate, again in the NVT ensemble at 2500 K for 0.5 ns. In this instance a reduced time step of 0.2 fs is employed due to the presence of H. The systems were quenched as above.

B. Generating c-Si/SiN_x:H interfaces

In order to generate clean and gradual interface structures two different procedures were followed. To generate the clean interface, the amorphous sample was placed in a cell at the (100) surface of a 20 layer thick slab of c-Si. The a-SiN_x was placed 2.5 Å away from this surface and dynamics were performed at 2500 K for 0.1 ns, with the c-Si held in position. The a-SiN_x layer was then gradually moved closer to the surface, each time repeating the procedure until the energy of the system started to increase relative to the previous step. Having thus identified the minimum energy separation, the top two layers of the c-Si were un-locked (as illustrated in Fig. 2) and dynamics were performed for a further 0.5 ns at 2500 K. The system was then quenched at the same rate as previously to 350 K, where dynamics were performed for a further 0.5 ns to generate statistics.

To generate the system with the gradual interface, the minimum energy separation from the previous step was again used. In this instance, however, the top 10 layers of c-Si were unlocked before performing the dynamics at 2500 K. This results in the N atoms from the SiN_x penetrating into the c-Si layer, which also melts and becomes distorted. After 0.5 ns at 2500 K the system is annealed to 350 K as described above, and run for 1 ns at 350 K to generate statistics.

All bond pattern analyses were performed using the R.I.N.G.S. code.[27] During this analysis two atoms are said to be bonding if the interatomic separation is within the first peak of the partial radial distribution function.

III. RESULTS AND DISCUSSION

A. Bulk amorphous SiN_x

All total and partial RDFs for the bulk samples of SiN_x at each value of x are shown in Fig. 3. As the value of x

Downloaded 02 Jul 2012 to 130.112.1.3. Redistribution subject to AIP license or copyright; see http://jap.aip.org/about/rights_and_permissions

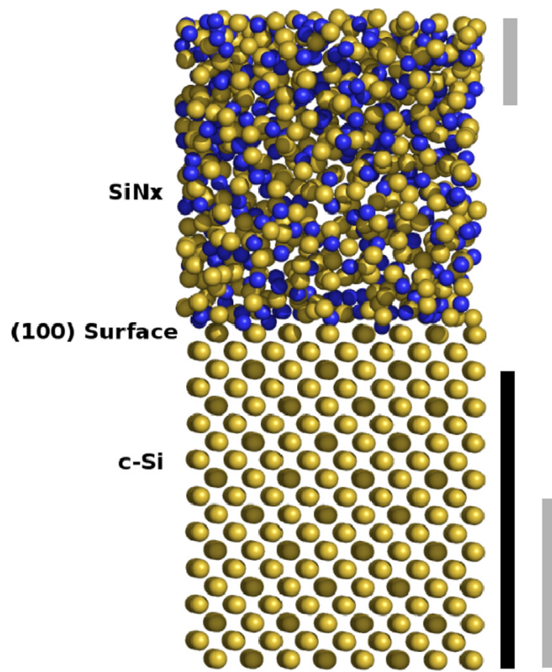

FIG. 2. (Color online) Simulation cell setups for creating clean and gradual interfaces. The lines to the right indicate the z coordinates over which atoms are frozen during interface generation. The dark line is c-Si frozen during clean interface generation, the gray line is c-Si frozen during gradual interface generation. The line at the top represents a-SiN_x frozen during all simulations.

increases, the first peak of the total RDF, which occurs at 1.80 Å, increases systematically, having values of 2.09, 2.20, 2.22, 2.25, and 2.26 at $x = 0.8$, 0.9, 1.0, 1.1, and 1.2, respectively. It is clear from comparison with the partial RDFs that this peak is due to the first peak of the Si-N RDF. As x increases the first peak of the Si-Si RDF, at around 2.5 Å, is also seen to decrease dramatically due to the fact that N atoms replace Si atoms as nearest neighbors in the amorphous network. In the N-N RDF there are no N-N nearest neighbor pairs. This is because the N-N interaction within the potential parameterization used is set to zero and is also representative of the physical situation, where N-N bonds

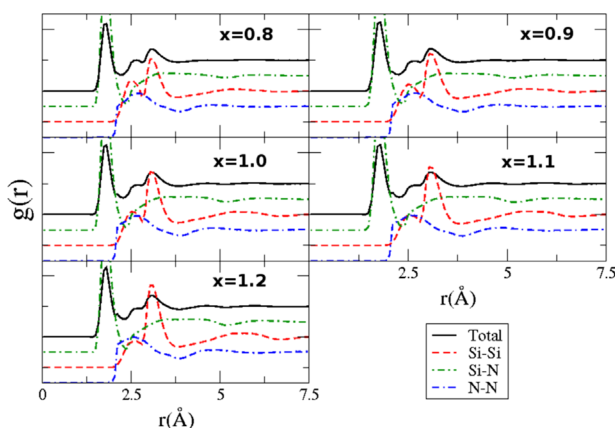

FIG. 3. (Color online) Total and partial radial distribution functions of a-SiN_x samples at values of x from 0.8–1.2. Note that individual RDFs have been offset by 0.5 on the y axis for clarity.

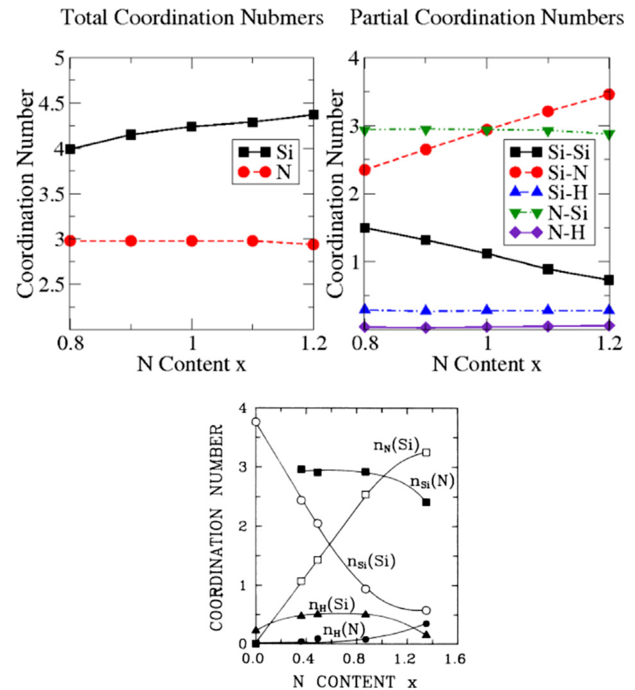

FIG. 4. (Color online) Upper: Total and partial coordination numbers for Si and N atoms from simulation. A-B means the number of atoms of B bonded to center A. Lower: Partial coordination numbers from the experimental study of Guraya *et al.* (Ref. 29) Reprinted with permission from M. M. Guraya, H. Ascolani, G. Zampieri, J. I. Cisneros, J. H. Dias da Silva, and M. P. Cantão, Phys. Rev. B **42**, 5677 (1990). Copyright 1990, American Physics Society. n_B (A) refers to the number of atoms of B bonded to center A.

would result in molecules of N, which would not be incorporated into the a-SiN network.

The RDFs obtained from our simulations are much closer in character to those obtained by Alvarez and Valladares using first principles simulations[28] than those obtained using the same Tersoff potential as ourselves produced by de Brito Mota *et al.*[24] We believe that this is due to the fact that the methodology that we have used to produce the a-SiN_x is much closer to the annealing methodology of the former than the Monte-Carlo based methodology of the latter. This gives us an increased degree of confidence in the ability of this Tersoff parameterization to simulate the properties of a-SiN_x.

We now compare the bonding patterns from our simulations with the experimentally determined values.[29] We note that in this case we are comparing the results of our simulations that include hydrogen to the experimental results as they are also measured in the presence of hydrogen. Figure 4 shows the total coordination numbers of Si and N in the various SiN_x:H samples as x increases, we concentrate on the range $x = 0.8$–1.2, while the experimental results of Guraya *et al.*[29] (Fig. 4) cover a much wider range. In the graph of the partial coordinations, the pairs A-B represent the number of atoms B bonded to atom A. In this case the atoms are said to be bonded if the interatomic separation is within the first peak of the partial RDF. These results are presented with the experimentally determined values of Guraya *et al.*, who obtained the values from x-ray photoemission spectroscopy.

Our bonding patterns match very well with the experimental data. We observe in our simulations that N and H bond almost entirely to Si, with very low quantities of N-H

Downloaded 02 Jul 2012 to 130.112.1.3. Redistribution subject to AIP license or copyright; see http://jap.aip.org/about/rights_and_permissions

and N-N bonding, as observed in the experimental data. Also we observe that the number of N atoms bonding to a Si center increases in a linear manner with the value of x. Conversely the number of Si atoms bonded to a Si center decreases linearly with increasing x. This is an indication that the Si nearest neighbors in the network are replaced by N atoms as x increases. As in previous theoretical and experimental studies the coordination of the N atoms is largely unaffected by the varying x.[24,28,29]

The above results demonstrate that using our melting and quenching regime we can generate reliable a-SiN_x:H structures. The trends observed in bonding patterns and the RDFs are in excellent agreement with previous *ab initio* and experimental studies.[28,29] We now proceed to use the samples thus generated and the methodologies established in order to model the interface between a-SiN_x:H and the c-Si(100) surface.

B. Clean c-Si/SiN_x:H interfaces

We first examine interfaces in which there is an abrupt change in the N concentration at the interface with c-Si, which we refer to as clean interfaces. For this analysis we consider the SiN_x:H layer within 1 nm of the c-Si layer. In Fig. 5 we can see that at $x = 0.8$ the total coordination number of Si is roughly the same as that in the bulk sample, however as x increases, although the coordination of Si does increase, this increase is not as pronounced as in the bulk sample. The coordination number of N remains constant as x increases, as was observed in the bulk samples. However, the coordination number of N is slightly decreased with respect to bulk samples by ∼0.1. While these changes may seem minor, closer inspection of the bonding patterns, from the partial coordination numbers, reveals a significant difference in bonding. The number of nearest neighbor N atoms for each Si center is decreased with respect to bulk, varying from 1.6 to 2.5 across the range of x values. N coordination is again largely accounted for by Si atoms, with a slight increase in the number of N-H bonds. The values for Si-H are very similar to those in the bulk SiN_x:H.

We now consider the presence of bonding defects that are important in solar-cells in terms of electrical performance. The two states in particular that we consider are the K and N defects that were described in the Introduction. In addition passivation of these defects by H is very important, therefore we consider how these defects are passivated in our simulations. The results are presented in Table II. Considering the total density of K-defects, the most striking feature is that there is a sharp increase in this number after $x = 1.1$. It is interesting to note that this change occurs at the percolation limit of SiN_x,[30] at which point the properties of SiN_x:H are known to alter in a non-linear fashion with varying x.[31] These results match well with the observation that above the percolation limit, the density of Si dangling bonds can increase.[30] The presence of H leads to a passivation of these dangling bonds by bonding of the H to the under-coordinated Si center. The results in Table II indicate that, in the presence of 20 atomic % H, between 30 and 40% of the K defects at the interface are passivated in our simulations.

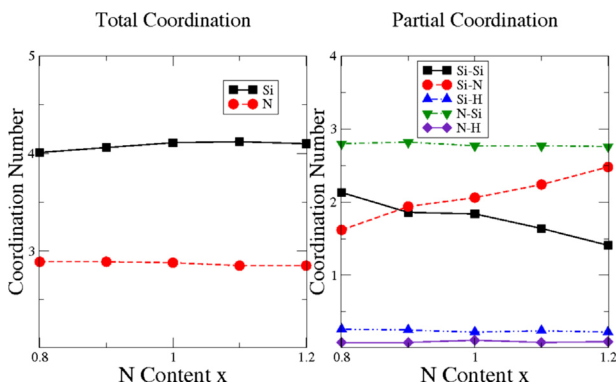

FIG. 5. (Color online) Total and partial bond densities in SiN_x close to the clean interface with c-Si as a function of nitrogen content (x).

The density of N defects shows a similar large jump to the K defect density, however this occurs at $x = 1.0$, slightly before the percolation limit. We note, however, that below the percolation limit defects on N centers are unlikely to be noticeable as the band structure is dominated by Si bands and the N defect state is not in the bandgap.[30] Interestingly, the N defects are passivated to a greater degree, between 40 and 50%, than the K centers. This is despite the fact that, from Fig. 5, the degree of Si-H bonding is greater than the degree of N-H bonding, indicating that H bonds more selectively to under-coordinated N than under-coordinated Si. This supports the hypothesis that the reduction in density of paramagnetic Si dangling bonds observed upon increasing annealing temperature is a result of charge transfer between paramagnetic defects, rather than the passivation of dangling Si bonds by hydrogen.[32]

The results show that producing a SiN_x:H layer with a stoichiometry optimized for optical performance (i.e., larger values of x) does not necessarily lead to a layer with optimal electrical properties. This, coupled to the fact that lower values of x are desirable for the role of SiN_x:H as an ARC, means that a balance must be found to optimize optical and electrical properties. This conclusion is in line with that of Jung *et al.*,[15] who suggest that stoichiometric values result in more effective devices than either high or low extremes of x.

C. Gradual c-Si/SiN_x:H interfaces

Thus far we have considered only clean interfaces where there is an abrupt drop in the N concentration at the c-Si surface. In reality there is often a layer of gradual depletion of the N concentration. The width of this layer varies significantly depending on the deposition method, and can also

TABLE II. Defect concentrations, in $10^{21}/cm^3$, at the clean interfaces across the x range in SiN_x:H. p refers to passivated meaning the defect has a H atom bonded, t refers to total and is passivated plus un-passivated centers.

x	0.8	0.9	1.0	1.1	1.2
K^t	9.3	18.0	17.9	29.0	33.6
K^p	3.6	5.5	6.1	12.3	12.1
N^t	17.8	19.3	27.7	27.8	32.6
N^p	7.6	8.5	13.2	11.2	12.8

Downloaded 02 Jul 2012 to 130.112.1.3. Redistribution subject to AIP license or copyright; see http://jap.aip.org/about/rights_and_permissions

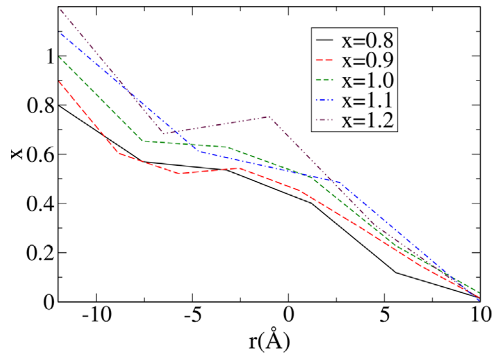

FIG. 6. (Color online) Value of x in SiN_x across the various simulated interfaces. r is the coordinate orthogonal to the interface and the c-Si layer is located at $r = 10$ Å.

vary within a single sample. However, this layer is typically between 1-3 nm wide. In order to simulate the effect such a gradual depletion may have on the structure of the SiN_x:H and the interface we consider a number of systems that were setup as described in the methods section. We should point out that in the case of the simulations, the width of the layer is restricted to around 2 nm (Fig. 6), which we choose as being representative of the experimental range. We are aware, however, that the slope and width of the gradient may play an important role in determining the structure in this region, the effect of the width shall be considered in future studies. For now we shall restrict ourselves to establishing the difference in structure between the clean and gradual interfaces.

As was the case for the clean interface, the total Si coordination number (Fig. 7) is similar to the bulk at $x = 0.8$, and remains more or less constant across the stoichiometry range. At the gradual interface the coordination number of N is very similar to that in the bulk samples, and again is due to three Si atoms coordinated to the N center (Fig. 7). The number of N atoms bonded to each Si center is decreased with respect to the bulk and clean interface values, obviously due to a lower N content near the interface with c-Si in the gradual interface system. The hydrogen coordination numbers to both Si and N are reduced with respect to both the bulk and the clean interface, suggesting that the degree of passivation of dangling bonds may be reduced in a gradual interface. We

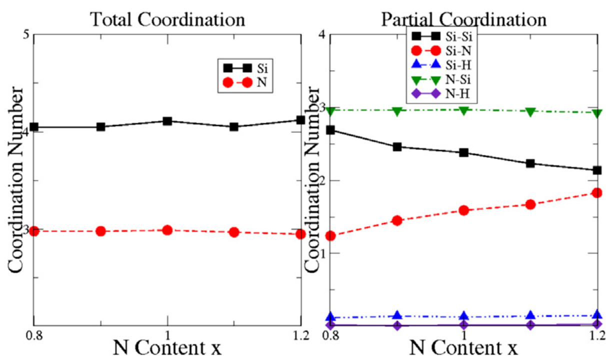

FIG. 7. (Color online) Total and partial bond densities in SiN_x close to the interface with c-Si as a function of nitrogen content (x) in systems with a N gradient.

TABLE III. Defect concentrations, in $10^{21}/cm^3$, at the gradual interfaces across the x range in SiN_x:H. p refers to passivated meaning the defect has a H atom bonded, t refers to total and is passivated plus un-passivated centers.

x	0.8	0.9	1.0	1.1	1.2
K^t	9.6	10.8	7.1	14.7	13.6
K^p	1.7	1.4	2.0	2.3	2.8
N^t	3.2	2.7	3.2	5.3	8.8
N^p	1.9	1.2	1.7	2.2	3.3

now consider this specifically relating to the K and N defects.

Table III presents the density of K and N defects found in the gradual interface systems. The total density of K-defects at $x = 0.8$ is slightly greater in the gradual interface than the clean interface. However, as we go to larger values of x the total density does not increase as rapidly as in the clean interface systems. Thus, for all values of $x > 0.8$ the total density of K-defects is reduced in the gradual interface. As suggested by the coordination numbers, the degree of passivation of K-centers is significantly reduced in the gradual interface ranging between 15 and 30%. However, despite the reduction in the degree of passivation, the density of un-passivated K-defects is still lower in the gradual interfaces compared to the clean ones for all values of $x > 0.8$. The total density of N defects, on the other hand, is greatly reduced across the composition range. This is because the density of N defects within 1 nm of the c-Si is reduced in the gradual interface and the coordination numbers suggested that N centers were more fully bonded in the gradual than in the clean interface. This indicates that, in addition to improved optical performance, the gradual interface can be expected to have improved electrical performance to the clean interface.

Moreover, the low values of x close to the c-Si layer would result in improved ARC properties. Thus our simulations provide clear evidence that a N gradient across the boundary from SiN_x to c-Si improves the optical properties of the layer by both reducing absorption and increasing light trapping, while also improving electrical properties by reducing the number of carrier traps at the interface.

IV. CONCLUSIONS

In this paper we have demonstrated that using the Tersoff potential the structure of a-SiN_x can be simulated in excellent agreement with *ab initio* and experimental structures. We demonstrate that using a methodology based on melting the sample and quenching it a better representation of the true amorphous structure can be obtained compared to previous studies that used Monte-Carlo methods to generate a-SiN_x using the Tersoff potential.[24]

We have then used this methodology to simulate SiN_x interfaces with the c-Si(100) surface. We have simulated this as both a clean interface and with a gradient of N concentration across the boundary. To our knowledge this is the first systematic theoretical examination of the effect of SiN_x stoichiometry on the structure of the SiN_x/c-Si interface, as well as the first time a system with a N gradient across the

Downloaded 02 Jul 2012 to 130.112.1.3. Redistribution subject to AIP license or copyright; see http://jap.aip.org/about/rights_and_permissions

interface has been modeled atomistically. The results of the simulations have implications for future optimization of the SiN_x layer in high performance c-Si solar cells.

The simulations reveal that in the case of a clean interface higher values of x in SiN_x would be expected to improve optical properties of the ARC, but may adversely affect the electrical properties due to increased densities of both K- and N defects at the interface, although these centers are to some extent passivated by the presence of H. The increased density of K-defects is particularly pronounced at SiN_x compositions with $x \geq 1.1$, which is also the percolation limit of SiN_x. These findings agree with previous work that showed that Si defects can increase in density above the percolation limit.[30] This finding also agrees with recent experimental work that found that stoichiometric values of $x = 1$ offer the best performance, compared to extreme values.[15] Finally we have shown that a gradient interface results in fewer electron traps, namely the N and K center defects in the interface region.

ACKNOWLEDGMENTS

The authors acknowledge support from the European Commission Grant No. MMP3-SL-2009-228513, "Hipersol" as part of the 7th framework package, Grant No. 228513. In addition, we would also like to thank our reviewer for an insightful critical reading of the original manuscript.

[1]R. Hezel and R. Schroner, J. Appl. Phys. **52**, 3076 (1981).
[2]R. Hezel and K. Jaeger, J. Electrochem. Soc. **136**, 518 (1989).
[3]H. Ahn, C.-L. Wu, S. Gwo, C. M. Wei, and Y. C. Chou, Phys. Rev. Lett. **86**, 2818 (2001).
[4]G. L. Zhao and M. E. Bachlechner, Phys. Rev. B **58**, 1887 (1998).
[5]M. L. Colaianni, P. J. Chen, N. Nagashima, and J. J. T. Yates, J. Appl. Phys. **73**, 4927 (1993).
[6]H. D. Goldbach, V. Verlaan, C. H. M. van der Werf, W. M. Arnoldbik, H. C. Rieffe, I. G. Romijn, A. W. Weeber, and R. E. I. Schropp, Amorph. Nanocrys. Silicon Sci. Technol. **862**, 293 (2005).
[7]P. Grunow and S. Krauter, "Modelling of the encapsulation factors for photovoltaic modules," in *Photovoltaic Energy Conversion, Conference Record of the 2006 IEEE 4th World Conference on*, Vol. 2 (2006), pp. 2152–2155.
[8]T. Takakura, R. Imai, Y. Okamoto, and H. Taniguchi, Jpn. J. Appl. Phys. **49**, 046502 (2010).
[9]A. G. Aberle and R. Hezel, Prog. Photovolt. **5**, 29 (1997).
[10]H. Nagel, A. G. Aberle, and R. Hezel, Prog. Photovolt. **7**, 245 (1999).
[11]I. O. Parm, K. Kim, D. G. Lim, J. H. Lee, J. H. Heo, J. Kim, D. S. Kim, S. H. Lee, and J. Yi, S0l. Energ. Mat. Sol. C. **74**, 97 (2002).
[12]W. Soppe, H. Rieffe, and A. Weeber, Prog. Photovolt. **13**, 551 (2005).
[13]V. Verlaan, C. H. M. van der Werf, Z. S. Houweling, I. G. Romijn, A. W. Weeber, H. F. W. Dekkers, H. D. Goldbach, and R. E. I. Schropp, Prog. Photovolt. **15**, 563 (2007).
[14]J. Yoo, S. Kumar Dhungel, and J. Yi, Thin Solid Films **515**, 7611 (2007).
[15]S. Jung, D. Gong, and J. Yi, Sol. Energ. Mat. Sol. C. **95**, 546–550 (2011).
[16]X.-S. Wang, G. Zhai, J. Yang, and N. Cue, Phys. Rev. B **60**, R2146 (1999).
[17]G. Zhai, J. Yang, N. Cue, and X. S. Wang, Thin Solid Films **366**, 121 (2000).
[18]P. Aubert, H. J. von Bardeleben, F. Delmotte, J. L. Cantin, and M. C. Hugon, Phys. Rev. B **59**, 10677 (1999).
[19]N. Ikarashi, K. Watanabe, and Y. Miyamoto, J. Appl. Phys **90**, 2683 (2001).
[20]P. M. Lenahan and S. E. Curry, Appl. Phys. Lett. **56**, 157 (1990).
[21]W. L. Warren, P. M. Lenahan, and S. E. Curry, Phys. Rev. Lett. **65**, 207 (1990).
[22]G. Pacchioni and D. Erbetta, Phys. Rev. B **60**, 12617–12625 (1999).
[23]J. Tersoff, Phys. Rev. Lett. **56**, 632 (1986).
[24]F. de Brito Mota, J. F. Justo, and A. Fazzio, Phys. Rev. B **58**, 8323 (1998).
[25]F. de Brito Mota, J. F. Justo, and A. Fazzio, J. Appl. Phys. **86**, 1843 (1999).
[26]W. Smith and T. R. Forester, J. Mol. Graphics **198/199**, 796 (1996).
[27]S. L. Roux and P. Jund, Comp. Mater. Sci. **49**, 70 (2010).
[28]F. Alvarez and A. A. Valladares, Phys. Rev. B **68**, 205203 (2003).
[29]M. M. Guraya, H. Ascolani, G. Zampieri, J. I. Cisneros, J. H. Dias da Silva, and M. P. Cantão, Phys. Rev. B **42**, 5677 (1990).
[30]J. Robertson, Philos. Mag. B **69**, 307 (1994).
[31]F. L. Martínez, A. del Prado, I. Mártil, G. González-Díaz, B. Selle, and I. Sieber, J. Appl. Phys. **86**, 2055 (1999).
[32]F. L. Martínez, A. del Prado, I. Mártil, D. Bravo, and F. J. López, J. Appl. Phys. **88**, 2149 (2000).

Downloaded 02 Jul 2012 to 130.112.1.3. Redistribution subject to AIP license or copyright; see http://jap.aip.org/about/rights_and_permissions